The electron density of the solar corona

Hulst, H.C. van de

BULLETIN OF THE ASTRONOMICAL INSTITUTES OF THE NETHERLANDS

1950 FEBRUARY 2 VOLUME XI NUMBER 410

COMMUNICATIONS FROM THE OBSERVATORY AT LEIDEN

THE ELECTRON DENSITY OF THE SOLAR CORONA

BY H. C. VAN DE HULST

This paper presents a new discussion of the brightness, electron density and polarization of various parts of the corona. Since these quantities have rather complex interrelations, some tables giving mutually consistent values of these quantities have been prepared. These tables are called the 'model corona'; it is hoped that future changes will be small and their discussion will require little effort.

The computation of the model starts from the brightness data collected by BAUMBACH. New absolute values are computed, based exclusively on photo-electric measures of the total corona. The same measures suggest that the brightness in maximum phase is 1·8 times the brightness in minimum phase. The brightness in the polar regions at minimum phase is treated separately. The F-corona, or inner zodiacal light, is eliminated on the basis of observations of Fraunhofer lines.

The dependence of brightness and polarization on the electron densities, as derived by SCHUSTER and MINNAERT is reviewed. A method for computing the polarization and electron densities from the given brightness is discussed. It involves successive steps and thus avoids BAUMBACH's approximation, which is shown to give errors up to 18 per cent. The results are shown by Table 5.

The density above the pole can be determined from the brightness distribution along tracings perpendicular to the polar axis. These data are obtained from specially prepared copies of several Lick Observatory photographs of the 1900 corona. Solution of an integral equation then gives the electron densities in a plane perpendicular to the polar axis. When these densities are reduced to the common distance, $r = 1{\cdot}15$, from the sun's centre, a graph of the electron density as a function of heliographic latitude is obtained (Figure 7B). The polar corona appears to be separated from the equatorial corona by a density minimum near $\beta = 70°$. This dependence on latitude is unlike that of any other solar phenomena.

The observed polarization matches the computed polarization in broad lines but some discrepancies are seen. Computational errors are below one per cent. Various explanations are discussed. The explanations finally suggested are that the polarization in the outer corona has been found too high on account of an overcorrection for sky light. Further, the adopted brightness for the F-corona may have to be reduced in the inner corona, especially for the polar regions.

1. *Introduction.*

The solar corona has long been one of the chief mysteries of astrophysics. Due to the pioneer work of many investigators, culminating in LYOT's invention of the coronagraph and EDLÉN's identification of the emission lines, it now has lost some of its secrets. Yet the problems relating to the heating of the corona and to its structural details still remain very puzzling. Most often we assume that the corona gas is fairly homogeneous and approximately at rest. To this simplified picture radio-astronomers have given the name 'quiet corona'. Any study of the changes in the corona and its streamers, and also the planning of suitable eclipse observations, has to rely on our knowledge of the quiet corona. For those reasons the present study of the quiet corona was undertaken.

The light of the corona consists of three parts: 1) The emission lines are forbidden transitions of highly ionized metals; they have a total intensity of about one half per cent of the integrated light[1]). 2) The major part has a continuous spectrum and is sunlight scattered by the free electrons of the corona. 3) The outer part merges into a general haze around the sun that may be identified with the inner zodiacal light.

This paper deals with the second and major part. Reliable photometry of this part is still confined to total eclipses. The first calculations of the polarization and brightness distribution to be expected from the scattering by free electrons were made by SCHUSTER[1]). Several corrections were made by later authors and a comprehensive discussion with newly computed tables was given by MINNAERT[2]). A compilation of observational data from many eclipses was made by BAUMBACH[3]); his list of electron densities has become a standard reference.

BAUMBACH's work is known to contain several approximations. First the F-corona (inner zodiacal light), the importance of which has only recently become clear[4]), was not removed from the photometric data so that the electron densities in the outer parts turned out too high. Further the electron densities were derived by a short but not entirely correct method. And finally no attention was paid to the densities in the polar regions of the corona and to possible changes with the solar cycle.

1) F. W. DYSON and R. v. d. R. WOOLLEY, "Eclipses of the Sun and Moon", p. 143, Oxford, 1937.

1) A. SCHUSTER, *M. N.* **40**, 35, 1879.
2) M. MINNAERT, *Z. f. Ap.* **1**, 209, 1930.
3) S. BAUMBACH, *Astr. Nachr.* **263**, 121, 1937.
4) Y. ÖHMAN, *Stockholm Annaler* **15**, No. 2, 1947.
C. W. ALLEN, *M. N.* **106**, 137, 1947.
H. C. VAN DE HULST, *Ap. J.* **105**, 471, 1947.

The need for more accurate data has been felt in particular in investigations of the radio waves emitted by the sun. Most of the waves between wave lengths of 1 and 10 metre originate in the corona and since the square of the electron density enters in the opacity, fairly accurate values are required. For this purpose, corrections for the effect of the F-corona have already been made by several authors[1]). The removal of the other approximation and the computation of the degree of polarization is somewhat of a chore, because of the form of the integral equations involved. This renders it fairly difficult to make the so much needed critical discussion of all observational data that have a bearing on the electron densities. I decided, therefore, to compute tables giving mutually consistent values of brightness, polarization and electron densities, which fit the available data reasonably well. In the following these tables will be called the model corona. This name simply means that reasonable assumptions about the properties of the F-corona were made and that errors of computation larger than one per cent were avoided.

If present or future observations are compared with this model, the deviations will presumably be small and their discussion comparatively easy. A preliminary discussion of this kind is given in section 6. At the same time the model may facilitate the computation of expected readings of photo-electric measurements of certain sectors or rings of the corona during an eclipse.

The present investigation was incited by the opportunity I had to visit the Lick Observatory in March 1948. The Lick Observatory possesses a fine collection of large-scale corona photographs made at eclipse expeditions from 1893 to 1932. I am indebted to Dr C. D. SHANE, director, for the permission to examine these plates and to Mr F. L. CHAPPELL for making a number of positive copies. These are copies of selected photographs, made on Eastman 33 plates and on a scale suitable for use in a microphotometer. The originals taken with the 40-feet camera were reduced in size by a factor $4\frac{1}{2}$, bringing the diameter of the sun from 114 mm to 25·6 mm. Special care was taken to provide a photometrically even background; no detail was lost by the reduction. Contact copies were made of some originals taken with the Floyd camera; the solar diameter on these plates is 16·7 mm. This material has not yet been studied completely but some results are included in the following compilation.

1) A. UNSÖLD, *Die Naturwissenschaften* **34**, 194, 1947.
C. W. ALLEN, *M. N.* **107**, 426, 1947.
M. WALDMEIER and H. MÜLLER, *Astr. Mitt. Zürich*, Nos. 154 and 155, 1948.
H. C. VAN DE HULST, *Nature* **163**, 24, 1949.
Extensive computations of the radio emission from the corona were also made by J. F. DENISSE, *Thèse*, Paris, 1949, and by M. NICOLET.

2. *The Separation of the F- and K-components.*

Following GROTRIAN, we denote by K-corona the real corona, whose light is due to scattering by electrons, and by F-corona the spurious corona, whose light arises probably from diffraction by particles in interplanetary space. In the following K and F will denote the surface brightnesses of these components. As a unit we take 10^{-8} times the average surface brightness of the sun (BAUMBACH used 10^{-6} times the surface brightness at the centre of the solar disk). We neglect the contribution of the emission lines. The observations give the total surface brightness, $F + K$, and the observed polarization refers also to the combined light. It is therefore important to know the factor

$$f = \frac{K}{F+K}, \qquad (1)$$

by which the observed brightness has to be multiplied in order to obtain the brightness of the real corona.

The factor f is, like F and K, a function of the position and the wave length. We shall assume that both the K- and F-corona have the same color as the integrated light of the sun's disk. Actually, F is probably somewhat reddish[1]) (proportional to $\lambda^{1/2}$) and K has some irregularities in the continuous spectrum due to the smearing of the Fraunhofer lines [2]). Slight color differences in both the F- and the K-component close to the limb arise from the different degree of limb darkening of the sun in different wave lengths. These finer features will be neglected in the present survey.

There are three methods for deriving f.

The first method is based on the fact that the Fraunhofer lines have their full strength in the F-corona but are completely obliterated in the K-corona. Let r be the residual intensity in the centre of a Fraunhofer line, measured in terms of the intensity of the continuum. Then

$$1 - f = \frac{1 - r_{\text{corona}}}{1 - r_{\text{disk}}}. \qquad (2)$$

The second method is based on the assumption that the F-corona is unpolarized. The degree of polarization of the real corona, p_K, can be computed from Rayleigh's law of scattering, if the distribution of the electrons is known. Let the observed degree of polarization be p. Then

$$f = \frac{p}{p_K}. \qquad (3)$$

The third method is based on a direct use of equation (1) and may be used whenever an estimate of F may

1) ALLEN, *M. N.* **106** and VAN DE HULST, *Ap. J.* **105**, as cited.
2) V. TH. HASE, *Abastumani Bulletin* **7**, 73, 1943.

be made independently of the measured surface brightness, $F + K$. For

$$f = 1 - \frac{F}{F+K}.$$

Several assumptions about F may be made. It is plausible that the isophotes of the F-corona within a few solar radii from the centre are circular. On this assumption we may use the value of F obtained in the equatorial regions for determining f in the polar regions, and conversely. Deviations would occur only if the interplanetary matter were concentrated very closely (within a few solar radii) to the equatorial plane. Further there is no reason to believe that F changes systematically with the solar cycle, although accidental fluctuations may occur, depending on the amount of interplanetary dust that happens to be between the sun and the earth. As a first guess we may assume that F is constant in time; this assumption may be used to estimate the changes of f during different phases of the solar cycle.

All of the methods mentioned are based on assumed properties of the F-corona. These properties are increasingly uncertain, from method 1 to method 3. The consistent results that are obtained in the following reduction of observational data may be taken as an indication of their approximate correctness. Some apparent deviations are discussed in section 6.

3. *The Brightness Distribution.*

Absolute intensity. – Measurements of the absolute intensity of the solar corona have been made in two ways: by absolute calibration of the surface brightness on corona photographs, and by photoelectric or radiometric measurements of the brightness of the total corona. The first method will be left out of consideration here, because the difficulties involved in bridging a gap of 15 magnitudes by photographic means make it less reliable.

The so-called measurements of the total corona do not really give the total light but the integrated brightness of a ring. This ring is limited at the outside by the field of the photometer and at the inside by the limb of the moon. The values of r for the inner border may vary between 1·08 for the deepest eclipse possible and 1·00 for a nearly annular one. The moon screens in the former case 46 per cent of the K-corona at maximum phase, according to our computations.

NIKONOV[1]) has reduced the published results of six eclipse expeditions to the common values, $r = 1{\cdot}03$ and 6, for the inner and outer border of the observed ring. His correction factors were based on BAUMBACH's distribution of the relative brightness. The results show a distinct correlation with solar activity, as illustrated by Figure 1. The ordinates give the brightness of the ring (1·03; 6), where the unit is 10^{-6} times the sun's brightness. The abscissae are the phases in the solar cycle as defined by MITCHELL[1]), that is, they are 0 at the minimum and 1 at the maximum of solar activity and are taken to change linearly with time between these epochs. No distinction between the ascending and descending branch is made. The two squares in this figure denote the radiometric observations by NIKONOV. I have reduced them by a common factor to fit the other observations, which are photoelectric. Observations as well as theoretical calculations have indicated that the F-corona may be slightly reddish. If its brightness relative to the sun is proportional to $\lambda^{1/2}$, its relative brightness in the infra-red exceeds the visual one by a factor 2. The corresponding factor for the combined $F + K$ light may be 1·2 to 1·3. The actual factor by which the radiometric observations had to be lowered in order to match the photoelectric ones proved higher; no explanation for this excess has yet been offered. At any rate the relative position of the two squares in Figure 1 appears to support the other observations in suggesting a change of brightness with the solar cycle. I believe that this change by a factor of about 1·8 is real; there seems to be no reason to ascribe all of it to observational errors. The visual observations listed by DYSON and WOOLLEY[2]) show a similar trend, changing from 0·47 times full moon near minimum to 0·72 times full moon near maximum (this is 1·07 to 1·66 millionth of the sun). The photographic observations in the same list scatter a little more and show no system. Further observations, possi-

FIGURE 1

Total brightness of the corona between $r = 1{\cdot}03$ and $r = 6{\cdot}0$, as a function of phase.

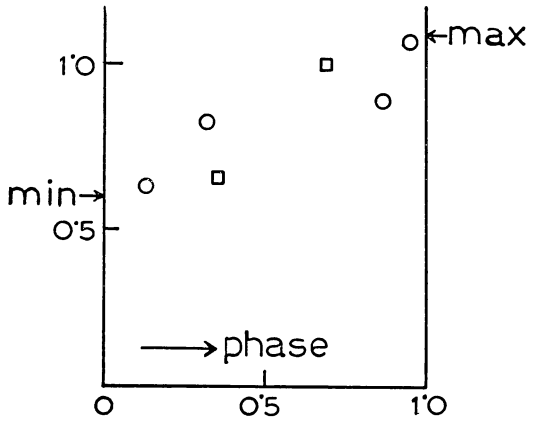

1) V. B. NIKONOV, *Abastumani Bulletin* **7**, 33, 1943; I studied this paper at Yerkes Observatory but have not found it in Holland. This explains some omissions in the following paragraph. See also note on page 163.

1) S. MITCHELL, *Hdbuch d. Ap.* **4**, 340, 1929 and **7**, 398, 1936.
2) *L. c.*, p. 125.

bly combined with a more critical discussion of earlier results, would seem highly desirable.

Part of the variation in total brightness is due to the wellknown fact that the polar regions of the corona in the minimum phase are relatively weak. This cannot, however, account for the entire change, so the surface brightness in the equatorial regions must vary also. We now assume the following model. The corona in the minimum phase has the surface brightness $K_{min}(r)$ in its equatorial regions and $K_{pole}(r)$ in its polar regions. The equatorial and polar regions are supposed to extend over sectors of 0·7 and 0·3 times the entire circumference of the sun, so that the weighted mean in the minimum phase is $0{\cdot}7\ K_{min}(r) + 0{\cdot}3\ K_{pole}(r)$. Further we assume that the corona at maximum phase has the surface brightness $K_{max}(r) = c\ K_{min}(r)$ and circular symmetry. For simplicity we assume that c does not change with r. Superposed on both maximum and minimum corona is the F-corona with the surface brightness $F(r)$.

The value of c may be estimated from the observed change of the total brightness, if the relative values of K_{pole}, K_{eq} and F from earlier investigations are used. Reading from Figure 1 the ratio $Q = 1{\cdot}7 \pm 0{\cdot}3$ between maximum and minimum, I found $c = 1{\cdot}66 \pm 0{\cdot}35$. In the finally adopted model [equations (5)-(9), below] I have chosen $c = 1{\cdot}78$. The corresponding values for the total brightness of the ring between $r = 1{\cdot}03$ and $r = 6$ are 1·102 and 0·596, indicated by arrowheads in Figure 1. They have the ratio $Q = 1{\cdot}84$. Details of the latter computation are given in Table 1. Perhaps the difference between the maximum and minimum phase is somewhat exaggerated by the adopted model.

TABLE 1

Total brightness of the model corona.

Range of r	K_{max}	K_{min}	K_{pole}	K'_{min}	F	$K_{max}+F$	$K'_{min}+F$
1·00 to 1·03	·266	·151	·098	·135	·011	·277	·146
1·03 to 6	·935	·525	·207	·429	·167	**1·102**	**·596**
6 to ∞	·012	·007	·000	·005	·081	·093	·086
Total: 1 to ∞	1·213	·683	·305	·569	·259	**1·472**	**·828**

Unit = 10^{-6} × the total brightness of the sun (or of a corresponding sector of the sun). K'_{min} is the weighted mean of polar and equatorial regions in the minimum phase.

Relative brightness distribution in the equatorial regions.

The basic material is BAUMBACH's [1]) compilation of the observed values of $F + K$. Further, GROTRIAN's[2]) measures obtained at the minimum eclipse of 1923 were taken as a measure for the fraction $f = K/(K+F)$.

FIGURE 2.

Mean deviations, in stellar magnitudes, of the measured surface brightness near $r = 3$ from the average curve adopted by BAUMBACH.

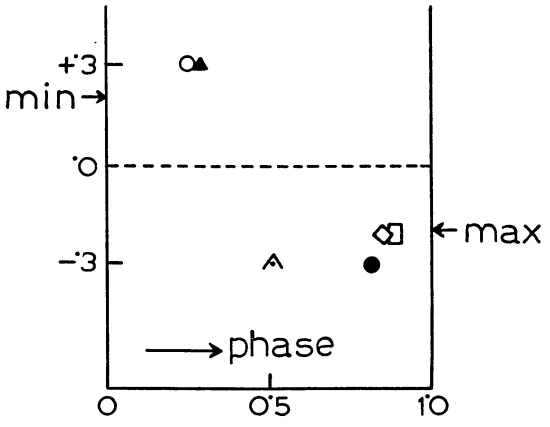

1) S. BAUMBACH, *Astr. Nachr.* **263**, 121, 1937.
2) W. GROTRIAN, *Z. f. Ap.* **8**, 124, 1934.

In an earlier paper[1]) I have extended these data to larger values of r by interpolating between the F-corona and the observed brightness of the inner zodiacal light.

In comparing the relative brightness distribution at different eclipses, BAUMBACH has made all curves coincide in the well-observed region near $r = 1{\cdot}2$. I estimated in BAUMBACH's graph the mean residuals for all single eclipses in the range $r = 2{\cdot}5$ to $4{\cdot}5$. Figure 2 shows these residuals as a function of the phase in the solar cycle (the symbols are the same as used by BAUMBACH). It strongly suggests that the decrease of brightness from the inner to the outer corona is somewhat steeper in the maximum phase than in the minimum phase. The difference may be explained by the relatively stronger K-corona in the maximum phase. If this explanation is accepted, the curves should not be made to coincide in the inner parts but rather in the outer parts, where the F-corona predominates. The fact that the observed difference is in the right direction and of the right order of magnitude is rather unexpected and not too much weight may be attached to it. On the other hand, a difference of 0·6 magnitudes, or a factor 1·8, should be well above the observational errors. The full change of the K-corona

1) *Ap. J.* **105**, 471, 1947.

between maximum and minimum should be even higher, because the inner corona still contains some F-light and the outer corona some K-light. The final model gives 1·45 (0·4 magn.) as the change of the brightness ratio between $r = 1{\cdot}2$ and $r = 3$, from minimum phase to maximum phase. The corresponding residuals are indicated by the arrowheads in Figure 2.

It is convenient to have expressions of the form $\sum_n C_n r^{-n}$ for K_{min}, K_{max}, and F. BAUMBACH has given the expression,

$$2{\cdot}56\, r^{-17} + 1{\cdot}43\, r^{-7} + {\cdot}053\, r^{-2{\cdot}5}, \qquad (4)$$

for the observed brightness distribution. We denote it by

$$(c^{1/2} K_{min} + F) \,/\, a.$$

Here a is a factor to be fixed by the data on absolute intensity above, and the K-term is just between the expressions K_{min} and cK_{min}, adopted for the minimum and maximum phase. I started the reduction by separating the K- and F-term by means of GROTRIAN's values for f and by finding formulae similar to (4) for the separate terms. Next, I multiplied the K-term with $c^{\frac{1}{2}} = 1{\cdot}33$, and $c^{-\frac{1}{2}} = 0{\cdot}75$ in order to obtain the expressions for maximum and minimum phase; the choice of $c = 1{\cdot}78$ was made on the basis of the data discussed above. The integrated brightness between 1·03 and 6 was then computed and an extra factor 0·82 applied to the K-integral in minimum phase. This factor, which represents the weakening of the polar areas, was estimated from a preliminary formula for the polar brightness and precisely confirmed by later computation on the finally adopted model (see Table 1). The results so obtained are comparable to the data of Figure 1, except for the factor a. The value $a = 104$ was found to give good agreement with Figure 1. If only the different choice of units, as explained in section 2, were involved, the factor would be $a = 125$. The fact that the actual value is lower means that BAUMBACH's absolute calibration was such that his values for the brightness are close to those for the maximum phase. The same holds for the resulting values of the electron density (section 5).

The final formulae are:

$$K_{max} = 355{\cdot}6\, r^{-17} + 177{\cdot}8\, r^{-7} + {\cdot}708\, r^{-2{\cdot}5}, \qquad (5)$$

$$K_{min} = 200{\cdot}0\, r^{-17} + 100{\cdot}0\, r^{-7} + {\cdot}398\, r^{-2{\cdot}5}, \qquad (6)$$

$$F = 14{\cdot}86\, r^{-7} + 4{\cdot}99\, r^{-2{\cdot}5}. \qquad (7)$$

The method used guarantees a good fit with the observations of relative brightness (somewhat better than BAUMBACH's) and with the absolute intensities. A check on the polarization and the determination of f is made in section 6.

Brightness distribution along the polar axis.

The most reliable photometry of the polar regions in minimum phase appears to have been made by BERGSTRAND[1]) at the eclipse of 1914. BERGSTRAND gives the brightness distribution along the equator and along the polar axis in arbitrary units. The data for the equator (which were also used by BAUMBACH) can be made to agree very well with our curve for $K_{min} + F$ by choosing the appropriate intensity unit. The units for $K_{pole} + F$ are then also fixed. Figure 3 shows the observations both for the equatorial and polar regions, together with the curves corresponding to the adopted model. In order to have data for one more eclipse I measured copies of several Lick Observatory photographs (see section 1) of the eclipse of 1900 with the microphotometer of the Yerkes Observatory. These plates were not calibrated. I assumed, however, that the brightness distribution in the equatorial regions agreed with the 'model' [sum of equations (6) and (7)]. So I made tracings due East and West and 30° North and South of these directions and used the mean of these six curves as a calibration curve. The mean of the tracings along the North and South polar axis then gave the values of the brightness shown by triangles in Figure 3. There is a fine agreement with BERGSTRAND's values. Although the 1900 plates show beautiful polar streamers, the photometric difference between the streamers and the background is so slight, that it was hardly noticeable on the tracings. Apparently the eye strongly overestimates the contrast; we shall return to this point below [2]).

Fortunately, it was possible to find an expression similar to equations (5)-(7) that agrees with the photometric data within the observational errors. The expression for $K_{pole} + F$ is:

$$191{\cdot}0\, r^{-17} + 27{\cdot}45\, r^{-7} + 4{\cdot}99\, r^{-2{\cdot}5} \qquad (8)$$

and by subtraction of equation (7):

$$K_{pole} = 191{\cdot}0\, r^{-17} + 12{\cdot}59\, r^{-7}. \qquad (9)$$

Figure 4 shows the combined brightness, $K + F$, and the separate components, both for the polar and the equatorial regions. It is curious that the contrast between the combined brightness in polar and equatorial regions goes through a maximum near $r = 1{\cdot}4$, where the ratio is about 2·5. This would seem very strange if the total brightness were due to electron scattering. The removal of the F-component removes this feature and makes the contrast increase all the way out. The values of K_{pole} for $r > 1{\cdot}5$ are very uncertain. The phenomenon mentioned above showed also in the investigations by LUDENDORFF [3]) and others on the

1) Ö. BERGSTRAND, *Etudes sur la distribution de la lumière dans la couronne solaire*, Stockholm, 1919.
2) H. C. VAN DE HULST, *B. A. N.* **11**, 150, 1950.
3) H. LUDENDORFF, *Sitzungsber. d. Preuss. Ak. d. Wiss.* p. 185, 1928 and p. 200, 1934.

FIGURES 3 en 4

(Upper part) Distribution of surface brightness in the corona near minimum phase. The triangles (Lick 1900) have been obtained by using the equatorial brightness for calibration. The curves refer to the 'model' corona. Ordinates are logarithms of the surface brightness.

(Lower part) Decomposition of the model corona at minimum phase into its various parts.

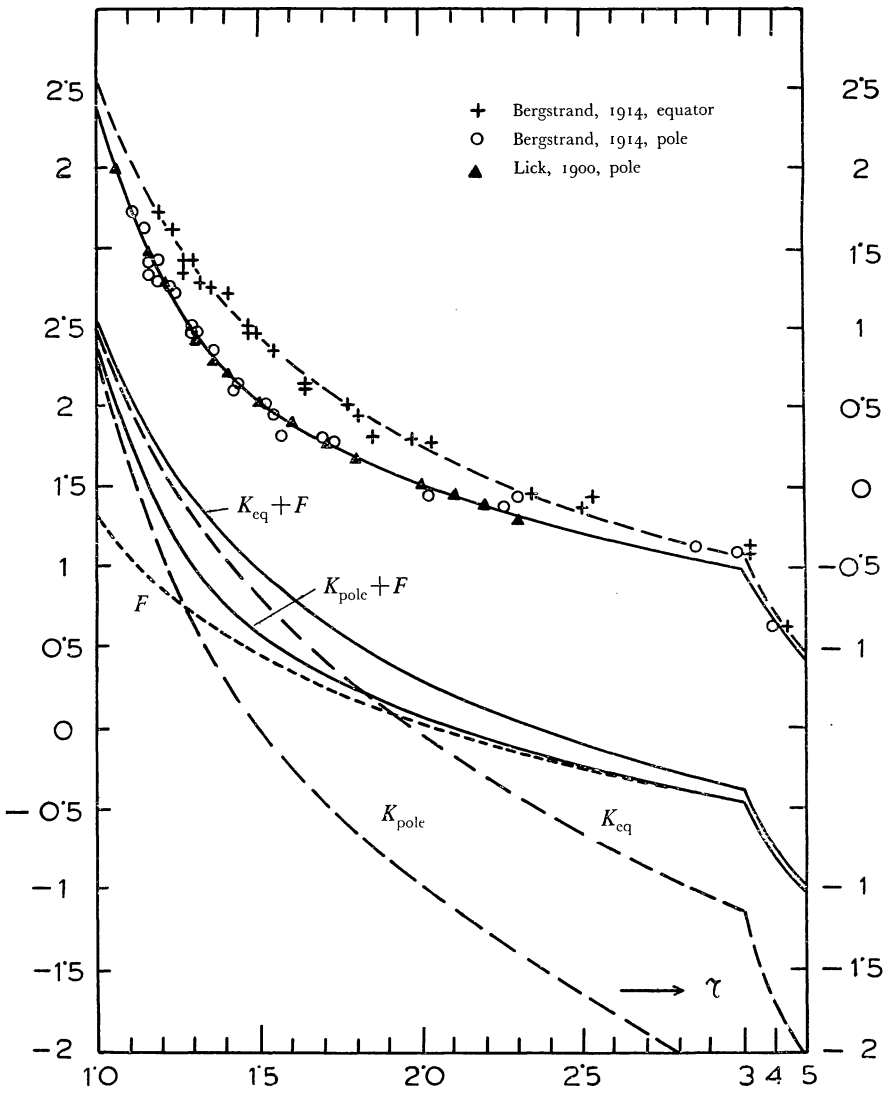

ellipticity of the isophotes: the isophotes tend to become more circular again for large values of r.

Numerical results. Some numerical values computed by means of equations (5)-(9) are shown in Table 2. The last columns show the corresponding values of f. The point where $f = 0{\cdot}50$ is the place where the K- and F-components are equally strong. This point is reached at $r = 2{\cdot}24$, $1{\cdot}93$, and $1{\cdot}28$, for 'max', 'min', and 'pole', respectively.

Total brightness. The total brightness of a ring between the radii r_1 and r_2 is $2\pi \int_{r_1}^{r_2} H(r)\, r\, dr$, where $H(r)$ is the surface brightness.

Making the same integration for the sun itself, we find π times its average surface brightness. Consequently a surface brightness of

$$H(r) = \sum_n C_n r^{-n}$$

times the average surface brightness of the sun gives rise to a total brightness that is

$$B = \sum_n (r_1^{-n+2} - r_2^{-n+2})\, 2C_n/(n-2) \qquad (10)$$

times the total brightness of the sun. Some results computed with this formula, where the values of C_n were taken from equations (5) to (9), are shown in Table 1.

TABLE 2

Surface brightness of the model corona

r	K			F	$K+F$			$f=K/(K+F)$		
	max	min	pole		max	min	pole	max	min	pole
1	534·1	300·4	203·6	19·9	554·0	320·3	223·5	·964	·938	·912
1·03	360·6	202·8	125·9	16·7	377·3	219·5	142·6	·955	·924	·884
1·06	251·2	141·3	79·3	14·2	265·5	155·5	93·5	·946	·909	·848
1·1	162·2	91·1	44·3	11·6	173·8	102·8	55·8	·933	·887	·792
1·2	66·2	37·1	12·1	7·3	73·6	44·4	19·4	·900	·836	·624
1·3	32·89	18·49	4·22	4·97	37·84	23·46	9·18	·869	·789	·459
1·4	18·41	10·35	1·82	3·56	21·97	13·91	5·38	·837	·745	·338
1·5	11·02	6·20	·93	2·68	13·70	8·88	3·61	·804	·698	·257
1·6	6·97	3·92	·53	2·09	9·06	6·01	2·63	·769	·652	·204
1·7	4·56	2·57	·33	1·68	6·24	4·24	2·01	·731	·604	·164
1·8	3·090	1·738	·215	1·390	4·470	3·128	1·603	·690	·556	·133
2·0	1·517	·852	·100	·998	2·515	1·850	1·097	·603	·461	·090
2·2	·811	·456	·051	·755	1·566	1·211	·806	·518	·376	·062
2·4	·468	·263	·027	·592	1·060	·855	·619	·440	·308	·044
2·6	·286	·161	·016	·476	·762	·637	·492	·375	·252	·032
2·8	·1858	·1045	·0093	·391	·495	·577	·400	·322	·209	·023
3·0	·1268	·0712	·0058	·327	·454	·398	·333	·279	·180	·018
3·5	·0585	·0329	·0020	·220	·279	·253	·222	·209	·129	·009
4·0	·0330	·0185	·0008	·157	·190	·176	·158	·174	·105	·005
5	·0149	·0084	·0002	·0889	·1038	·0973	·0891	·143	·086	·002
6	·0086	·0049	·0001	·0565	·0651	·0604	·0566	·132	·080	·001
8	·0040	·0023	·0000	·0275	·0315	·0298	·0275	·126	·075	·000
10	·0023	·0013	·0000	·0158	·0181	·0171	·0158	·125	·074	·000

Unit $= 10^{-8} \times$ average surface brightness of the sun. 'Max' refers to the maximum phase, 'min' to the equatorial regions in minimum phase, and 'pole' to the polar regions in minimum phase.

4. *Computation of the Polarization and Electron Densities.*

General equations. Let R be the sun's radius ($6{\cdot}97.10^{10}$ cm) and let us consider a point P at the distance rR from the sun's centre. Further, let H be the mean surface brightness of the sun and q the coefficient of limb darkening, so that

$$\frac{1-q+q\cos\alpha}{1-\frac{1}{3}q}H$$

is the surface brightness of a part of the sun's surface seen under an angle α with the normal. We shall write the density of illumination in P (i e. the intensity integrated over the entire solid angle subtended by the sun) in the form

$$\pi H\{2A(r)+B(r)\}.$$

This density of illumination is proportional to the mean square of the electric vectors of all light waves passing through P. We now define A as that fraction of $2A+B$ that is proportional to the mean square of the vector components in any transversal direction and B as the fraction proportional to the mean square of the vector components in the radial direction. Since B would be zero if the sun were a point source, it decreases rapidly with increasing r. At the same time A approaches the form $1/2\,r^{-2}$, as may be seen directly from the definition. SCHUSTER and MINNAERT[1]) have shown that the functions $A(r)$ and $B(r)$ may be found by elementary integration. The full expressions are:

$$2A+B=\frac{1-q}{1-\frac{1}{3}q}\left\{2(1-\cos\gamma)\right\}+$$
$$+\frac{q}{1-\frac{1}{3}q}\left\{1-\frac{\cos^2\gamma}{\sin\gamma}\log\frac{1+\sin\gamma}{\cos\gamma}\right\}; \quad (11)$$

$$2A-B=\frac{1-q}{1-\frac{1}{3}q}\left\{\frac{2}{3}(1-\cos^3\gamma)\right\}+$$
$$+\frac{q}{1-\frac{1}{3}q}\left\{\frac{1}{4}+\frac{\sin^2\gamma}{4}-\frac{\cos^4\gamma}{4\sin\gamma}\log\frac{1+\sin\gamma}{\cos\gamma}\right\}, \quad (12)$$

where $\sin\gamma = 1/r$. MINNAERT denotes the four quantities in square brackets by $\frac{1}{2}(3C-A)$, $\frac{1}{2}(3D-B)$, $\frac{1}{2}(C+A)$ and $\frac{1}{2}(D+B)$, respectively. Table 3 gives newly computed values for $q=0$, $q=1$ and $q=0{\cdot}75$. Only close to the limb is there any appreciable dependence on q. The further calculations are carried on with $q=0{\cdot}75$, corresponding to an effective wave length near 4700 A.

---

[1]) A. SCHUSTER, *M. N.* **40**, 35, 1879.
M. MINNAERT, *Z. f. Ap.* **1**, 209, 1930.

TABLE 3

Functions $A(r)$ and $B(r)$ relating to the density of illumination.

r	$q = 0$		$q = 1$		$q = 0{\cdot}75$			
	$2A + B$	$2A - B$	$2A + B$	$2A - B$	$2A + B$	$2A - B$	A	$A - B$
1	2·0000	·6667	1·5000	·7500	1·6667	·7222	·5972	·1250
1·03	1·5208	·6575	1·3132	·7258	1·3824	·7031	·5214	·1818
1·06	1·3366	·6423	1·1907	·7002	1·2393	·6809	·4800	·2008
1·1	1·1670	·6185	1·0641	·6660	1·0984	·6502	·4372	·2131
1·2	·8944	·5541	·8406	·5850	·8585	·5747	·3583	·2164
1·3	·7220	·4927	·6891	·5141	·7001	·5069	·3018	·2052
1·4	·6002	·4381	·5786	·4535	·5858	·4483	·2585	·1897
1·5	·5092	·3905	·4941	·4019	·4991	·3982	·2243	·1739
1·6	·4388	·3496	·4276	·3581	·4314	·3552	·1966	·1585
1·7	·3826	·3141	·3726	·3204	·3759	·3183	·1736	·1447
1·8	·3372	·2835	·3308	·2887	·3329	·2870	·1550	·1320
2·0	·2680	·2337	·2640	·2370	·2653	·2359	·1253	·1106
2·2	·2186	·1956	·2160	·1978	·2169	·1971	·1035	·0936
2·6	·1538	·1423	·1528	·1435	·1532	·1431	·0741	·0691
3·0	·1144	·1080	·1136	·1086	·1138	·1084	·0556	·0528
3·5	·0834	·0800	·0830	·0802	·0831	·0802	·0408	·0394
4	·0636	·0616	·0633	·0617	·0634	·0616	·0312	·0304
5	·0404	·0396	·0404	·0396	·0404	·0396	·0200	·0197
6	·0278	·0275	·0278	·0275	·0278	·0275	·0138	·0136
10	·01002	·00998	·01002	·00998	·01002	·00998	·00500	·00498

The vibrations of the free electrons induced by the incident radiation are distributed in a vibration ellipsoid with axes A, A and B. The light scattered by these electrons will accordingly have different intensities and degrees of polarization in different directions. Let $N(r)$ be the number of electrons per cm³ at P and σ the cross section of one electron for scattering ($\sigma = 0{\cdot}66.10^{-24}$cm²). The light scattered by one cm³ per second in all directions is

$$4\pi \bar{J} = \pi H (2A + B) \sigma N . \qquad (13)$$

Here $\bar{J}$ is sometimes called the source function (Ergiebigkeit), but it is only a mean source function. The specification for an arbitrary direction making an angle θ with the radius follows from simple geometry (see Figure 5). The source function for light vibrating perpendicularly to the plane through the sun's centre is

$$J_t = {}^3/_8 H N \sigma A (r) \qquad (14)$$

and for light vibrating in that plane it is

$$J_r = {}^3/_8 H N \sigma \{ A (r) \cos^2\theta + B (r) \sin^2\theta \} . \qquad (15)$$

The sum is $J = J_t + J_r$ and the integral of J over all directions gives again equation (13), because $\overline{\cos^2\theta} = {}^1/_3$, $\overline{\sin^2\theta} = {}^2/_3$.

The surface brightness in the projected image of the corona expressed in absolute units is: $10^8\ HK(x)$. Here x is written for the projected radius (where we used r in the last section). Let yR be the distance along the line of sight from the point closest to the sun. The light scattered per second per unit solid angle by a column with a cross section of 1 cm² now is

$$10^{-8} HK(x) = \int_{-\infty}^{+\infty} J(r)\, R\, dy. \qquad (16)$$

This gives

$$K(x) = C \int_x^\infty N(r) \left\{ \left(2 - \frac{x^2}{r^2}\right) A(r) + \frac{x^2}{r^2} B(r) \right\} \frac{r dr}{\sqrt{(r^2 - x^2)}} . \qquad (17)$$

FIGURE 5

Geometrical relation between the axes of the vibration ellipsoid (A, A, B) and the intensities of the scattered light (J_t, J_r).

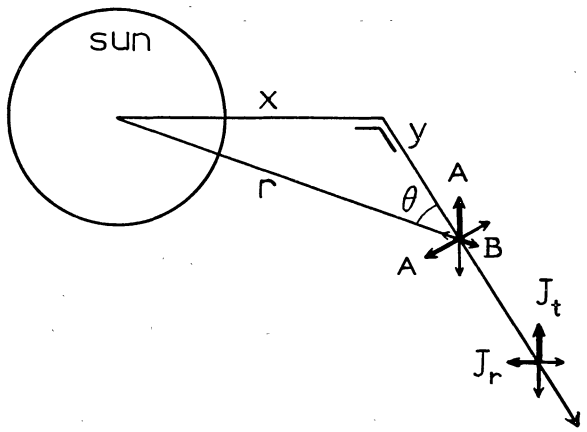

For the separate directions of polarization we obtain from (14) and (15):

$$K_t(x) = C \int_x^\infty N(r) A(r) \frac{r dr}{\sqrt{(r^2 - x^2)}} ; \qquad (18)$$

$$K_r(x) = C\int_x^\infty N(r)\left\{\left(1-\frac{x^2}{r^2}\right)A(r)+\frac{x^2}{r^2}B(r)\right\}\frac{rdr}{\sqrt{(r^2-x^2)}}. \quad (19)$$

A further useful equation is found by subtraction:

$$K_t(x) - K_r(x) = C\int_x^\infty N(r)\left\{A(r)-B(r)\right\}\frac{x^2dr}{r\sqrt{(r^2-x^2)}}. \quad (20)$$

In all these equations the constant is

$$C = {}^3/_4.10^8\, R\sigma = 3{\cdot}44\,.\,10^{-6}\ \mathrm{cm}^3\,. \quad (21)$$

Solution of the integral equations. The fundamental equations are equations (18) and (20). The problem is to divide the known function, $K_t(x) + K_r(x)$, in such a way between K_t and K_r that these two equations, when solved, yield the same function $N(r)$. It is probably safe to assume that the solution is unique and that in this way the brightness of the K-corona determines both its polarization and the electron densities.

BAUMBACH has made an approximate solution in two steps. In the first step the anisotropy of the radiation was neglected, which amounts to putting both A and B equal to ${}^1/_3\,(2A + B)$ in our equation (17). Our computations show that the electron densities thus obtained are too low by 1 to 18 per cent, as expressed by the factors b in Table 5A, B. In the second step BAUMBACH[1]) computed the exact polarization corresponding to these electron densities. SCHUSTER and MINNAERT made solutions starting from assumed electron distributions of the form $N(r) \sim r^{-n}$. If A and B are kept in analytical form, the corresponding K_t and K_r may be expressed in elliptical functions. But in order to obtain the observed function $K_t + K_r$ a trial and error procedure is needed[2]). I decided to use a method of successive approximations as follows.

First I computed by means of some preliminary set of values of $p(x)$ the functions

$$K_t = {}^1/_2(1+p)\,K \text{ and } K_t - K_r = pK, \quad (22)$$

and represented them as well as possible by sums of the type:

$$K_t = \sum_s h_s x^{-s} \text{ and } K_t - K_r = \sum_s k_s x^{-s}. \quad (23a,b)$$

Now one may verify by direct integration that the corresponding solutions have the form

$$rCN(r)\,A(r) = \sum_s \frac{h_s}{a_{s-1}} r^{-s} \quad (24a)$$

and

$$rCN(r)\left\{A(r)-B(r)\right\} = \sum_s \frac{k_s}{a_{s+1}} r^{-s}, \quad (24b)$$

where

$$a_n = \int_0^{\pi/2} \sin^n\varphi\, d\varphi = \frac{\pi}{2^{n+1}}\cdot\frac{n!}{\{({}^1/_2 n)!\}^2}.$$

TABLE 4

Values of the constants a_n.

n	a_n	n	a_n	n	a_n
0	1·5708	8	·4295	1·5	·8740
1	1·0000	9	·4064	3·5	·6243
2	·7854	10	·3866	8·7	·4129
3	·6667	11	·3696	10·7	·3743
4	·5890	12	·3544	16	·3085
5	·5333	13	·3411	18	·2913
6	·4909			33	·2166
7	·4571			35	·2104

Some numerical values of a_n are given in Table 4. The electron densities may now be computed both from equation (24a) and (24b). But, unless the right-hand members of these equations happen to have the correct ratio, $A/(A-B)$, for all values of r, the results will not be consistent, which means that the assumed $p(r)$ was not correct. Now we define the auxiliary functions, c_t and c_v, by

$$c_t = \frac{K_t(r)}{rCN(r)\,A(r)} \quad (26a)$$

and

$$c_v = \frac{K_t(r) - K_r(r)}{rCN(r)\,\{A(r)-B(r)\}}. \quad (26b)$$

Equations (23) and (24) show that c_t and c_v are 'effective values' of a_{s-1} and a_{s+1}. The two equations (26a, b) further lead to the relation

$$\frac{1}{p} + 1 = \frac{2A}{A-B}\cdot\frac{c_t}{c_v}. \quad (27)$$

It is plausible (and confirmed by successive approximations) that any preliminary solution which is not too bad gives fairly correct values of c_t and c_v by dividing the right-hand members of equations (23a, b) by those of equations (24a, b). A much better approximation to $p(r)$ is then computed by means of equation (27) and the procedure may be repeated.

In the last step one may avoid finding new expressions of the forms (23a, b) and take the following short cut. Let the preliminary solution be denoted by K_t' and $K_t' - K_r'$ and let the corresponding right-hand members of equations (24a) and (24b) have the ratio

$$(1+\varepsilon)\,\frac{A}{A-B},$$

where ε is a small number (not exceeding $\pm$ 0·05). We may then take the values of c_t and c_v obtained from this solution as the correct final values; a

[1]) S. BAUMBACH, *Astr. Nachr.* **267**, 273, 1939.
[2]) MINNAERT, *l. c.* p. 221.

little reduction gives the corrected values

$$K_t = \{1 + \varepsilon p\} K_t' \qquad (28a)$$

and

$$K_t - K_r = \{1 + \varepsilon(1+p)\} \{ K_t' - K_r' \}. \qquad (28b)$$

Division by the values of c_t and c_v already known, finally gives the correct values for $rCNA$ and $rCN(A-B)$, both of which now automatically give the same N.

The method described was found only after several unsuccessful attempts. Those attempts showed that errors of about 5 per cent in the resulting polarization are very easily made if a less careful method is used. I therefore decided to go through the somewhat tedious computations of the present method in order to reach an accuracy within 1 per cent.

Numerical results. Application of the method to the equatorial brightness in minimum phase, equation (6), gave the results shown by Table 5a. The approximation turned out to be sufficiently close to make $|\varepsilon| < 0{\cdot}02$ everywhere if $K(x)$ had the form $-17{\cdot}5x^{-3.4} + 132{\cdot}0x^{-17} - 22{\cdot}5x^{-9{\cdot}7} + 85{\cdot}2x^{-7} + {\cdot}31x^{-2{\cdot}5}$. For $r > 4$ the simpler form,

$$K_t(x) = 89x^{-7} + {\cdot}31x^{-2{\cdot}5},$$

suffices. Table 5a gives the results after the corrections

TABLE 5

Brightness and polarization of the K-corona; electron densities.

A. Equatorial regions.

r	$K_t + K_r$ min	K_t min	$K_t - K_r$ min	p	c_t	c_v	rCN min	N min	N max	b
1	300·4	177·4	54·4	·181	·380	·557	781	227×10^6	403×10^6	1·02
1·03	202·8	125·4	48·0	·237	·383	·420	632	178	316	1·04
1·06	141·3	90·2	39·1	·277	·390	·405	480	132	235	1·07
1·1	91·1	60·2	29·3	·323	·404	·405	340	90·0	160	1·07
1·2	37·10	26·12	15·14	·408	·445	·426	164	39·8	70·8	1·09
1·3	18·50	13·53	8·56	·463	·474	·441	94·8	21·2	37·6	1·10
1·5	6·20	4·77	3·34	·538	·495	·446	42·8	8·30	14·8	1·13
1·7	2·57	2·04	1·51	·588	·504	·446	23·4	4·00	7·11	1·14
2·0	·852	·692	·532	·625	·510	·446	10·84	1·58	2·81	1·14
2·6	·162	·134	·106	·658	·542	·461	3·34	·374	·665	1·15
3·0	·0711	·0587	·0463	·647	·577	·479	1·82	·176	·313	1·12
4·0	·0185	·0149	·0113	·607	·690	·534	·693	·050	·090	1·10
5	·0084	·0066	·0048	·575	·770	·571	·428	·025	·044	1·07
6	·0049	·0038	·0027	·565	·820	·595	·337	·016	·029	1·05

The values for maximum phase are found by multiplying the columns marked 'min' by 1·78; the columns not marked hold for minimum and maximum phase.

B. Polar regions in minimum phase.

r	$K_t + K_r$	K_t	$K_t - K_r$	p	c_t	c_v	rCN	N	b
1	203·6	119·6	35·5	·174	·334	·474	600	174×10^6	1·01
1·03	125·9	78·0	30·0	·238	·333	·367	450	127	1·04
1·06	79·3	50·8	22·3	·282	·333	·349	318	87·2	1·06
1·1	44·3	29·4	14·6	·330	·335	·340	201	53·2	1·07
1·2	12·1	8·5	5·0	·417	·353	·350	67·1	16·3	1·09
1·3	4·22	3·11	2·01	·476	·384	·369	26·7	5·98	1·11
1·5	·93	·71	·51	·555	·442	·406	7·3	1·41	1·14
1·7	·33	·26	·20	·600	·473	·423	3·17	·542	1·15
2·0	·100	·082	·064	·630	·485	·427	1·35	·196	1·16
2·6	·016	·014	·011	·693	·486	·428	·36	·040	1·17
3·0	·0058	·0050	·0041	·712	·488	·428	·18	·017	1·18
4·0	·0008	·0007	·0006	·748	·490	·429	·045	·004	1·18

have been applied by means of equations (28a, b). The remaining errors probably are under ½ per cent. The factors c_t and c_v, when plotted against r, do not define a perfectly smooth curve. This is due to the fact that the equation (6), with its three terms, does not define a perfectly smooth curve. The dents show in a somewhat enhanced form in c_t and c_v, and consequently in $N(r)$. They are practically absent in the ratio c_t/c_v and consequently in p. Before I started on this correct method, I had solved for the electron den-

sities by means of BAUMBACH's approximate method. The resulting values[1]) have to be multiplied by b in order to find the correct value given in Table 5A. The factors b are given in the last column.

The equations (17) to (20), solved in this section, hold only for the equatorial plane. So the determination of electron densities and polarization for the polar regions requires a different reduction (section 5). Yet a formal solution by means of the method of this section was also made for the polar regions and the results are given in Table 5B. It exemplifies some of the characteristics connected with a steeper decrease of density outward.

(1) The polarization in the outer corona is higher. In fact, for very large r we have single terms in equations (23) and (24), with $s = 7$, giving rise to the simple equations $p = s/(s+2) = \cdot 78$ and $b = {}^2/_3\,(p+1) = 1\cdot 18$.

(2) The polarization close to the limb is a little lower. The reason is that the volume elements along a given line of sight scattering the most strongly polarized radiation are not in the plane of projection but a little in back and in front of it. For instance, on the line $x = 1$, a volume element at $y = 0, r = 1$ gives $p = 0\cdot 12$, while elements at $y = \pm 0\cdot 7, r = 1\cdot 2$ give the maximum polarization $p = 0\cdot 26$. These maxima have less influence the faster the density decreases outward.

5. *The Electron Densities in the Minimum Phase as a Function of the Heliographic Latitude.*

Any line of sight that is not in the equatorial plane passes through regions of different heliographic latitudes. Accordingly, the procedure of the preceding section may be used only if $N(r)$ is the same function of r for all latitudes that are of importance. This assumption may be legitimate for points over the pole at $r > 1\cdot 20$. It is evidently incorrect for points just over the pole. For any photograph of the corona at minimum phase shows that fairly strong streamers of latitudes 45° to 60° extend above the plane $z = 1$. They must contribute, therefore, to the brightness just over the pole.

I made tracings on the Floyd plate of the 1900 eclipse perpendicular to the polar axis, as shown by the dotted lines of Figure 6. The tracings were made at $z = 1\cdot 04$, $1\cdot 08$ and $1\cdot 12$, both north and south, together with calibration tracings in the equatorial regions as explained in section 3. Surprisingly, there is not a big jump where one passes into the strong streamer but only a slight elevation, or just a less steep part in the general decrease of intensity outward. Since the different values of z showed a similar behaviour, I constructed average curves for $z = 1\cdot 08$.

[1]) These densities were published in *Nature*, *l. c.*

FIGURE 6

Schematic drawing showing the method for deriving the electron density above the pole.

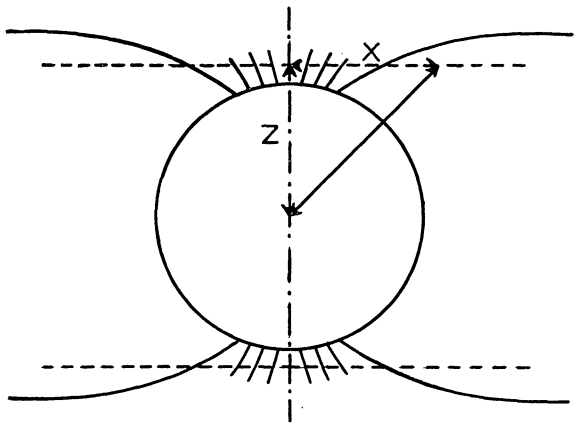

Table 6 shows the values for the NE and NW tracings; those for the SE and SW tracings are between them. K is the surface brightness with the F-component already removed.

The strict solution for the electron densities would be more complex here than in the equatorial plane. An approximate method, resembling BAUMBACH's method for the equatorial plane, was therefore used. As a first step the density distribution was computed on the assumption of isotropic scattering. The surface brightness, K, and the source function, J, are related by

$$K(x) = 2\int_x^\infty J(v)\,\frac{v\,dv}{\sqrt{(v^2-x^2)}}; \quad [k.x^{-s}]. \qquad (29)$$

TABLE 6

Surface brightness and source function in the plane $z = 1\cdot 08$.

x, v	r	β	K		J	
			NE	NW	NE	NW
0	1·08	90°	59	59	125	94
·1	1·08	85°	49	52	90	76
·2	1·10	80°	35	40	50	44
·3	1·12	75°	24	30	31	22
·4	1·15	70°	16	25	18	7
·5	1·19	65°	11	29	11	16
·6	1·24	61°	6·4	27	5·5	19
·7	1·29	57°	5·6	22	4·7	16·5
·8	1·34	53°	3·7	16·5	3·0	12·5
1·0	1·47	47°	2·0	9·0	1·4	6·5
1·2	1·61	42°	1·1	4·5	0·7	2·7
1·6	1·93	34°	0·5	1·5	0·2	0·7
2·0	2·27	28°	0·3	0·7	0·1	0·3

The well-known solution of this integral equation is

$$\left.\begin{aligned} P(x) &= -\frac{1}{x}\frac{dK(x)}{dx}; \qquad [p.x^{-s-2}], \\ J(v) &= \frac{1}{\pi}\int_v^\infty P(x)\,\frac{x\,dx}{\sqrt{(x^2-v^2)}}; \quad [j.v^{-s-1}]. \end{aligned}\right\} \qquad (30)$$

The expressions between brackets hold in case the data may be represented by a single power of r. The relations between the coefficients are

$$k = 2j a_{s-1}\,;\quad p = sk\,;\quad j = p\,a_s/\pi. \tag{31}$$

Here a_n is defined by (25). The relations (31) are mutually consistent because of the identity

$$a_n \,.\, a_{n-1} = \pi/2n. \tag{32}$$

The integral equation was solved by a rough graphical evaluation of equations (30); for the outer parts I used power approximations and the relations (31). The resulting values of J are shown by Table 6.

The electron density that follows from this analysis will be denoted by N'. By comparing equations (13), (16) and (29), we find

$$J = 10^8 R \frac{\sigma}{4}(2A + B)\, N', \tag{33}$$

so that

$$N' = 8{\cdot}75 \,.\, 10^5\, J/(2A + B)\,. \tag{34}$$

The second step takes the anisotropy of the scattered radiation into account. If N' were the correct electron density and J the corresponding mean source function, the correct brightness would be found by inserting a factor $m_t + m_r$ in the integrand of (29). Here t and r refer to the directions of polarization and equations (13) to (15) show that

$$m_t = \tfrac{3}{2}\frac{A}{2A+B}\,;\qquad m_r = \tfrac{3}{2}\frac{A\cos^2\theta + B\sin^2\theta}{2A+B}\,. \tag{35}$$

Numerical integrations showed that the brightness at the point $x = 0$, $z = 1{\cdot}08$ is reduced to 0·92 (NE), or 0·95 (NW) times its original value, as a consequence of this factor. With the neglect of second-order corrections, this means that the given surface brightness, K, is restored if we multiply the electron density N', found on the assumption of isotropic scattering, by a factor 1·08, or 1·05, respectively. This corresponds well with the factor 1·08 found from Table 5B. Similar integrations with the separate factors m_t and m_r in the integrand gave the polarized components. I found $p = {\cdot}30$ (NE) and ·29 (NW), as compared with ·30 for the case of spherical symmetry (Table 5B). Evidently, neither the factor b, nor the polarization, p, is sensitive to changes arising from the lack of spherical symmetry.

The same integrations show clearly to what extent the relation between surface brightness and electron density is complicated by the effect that the latter depends on latitude. The graphs show a dip near $y = {\cdot}4$, $\beta = 70°$, suggesting a separation between the contributions of high and low latitudes. The latter contribute 35 per cent of the total in the NE quadrant, while the solution corresponding to Table 5B gives 17 per cent. This would suggest that the values of N_e in Table 5B should be decreased by 10 to 20 per cent. But a stronger effect acts in the opposite direction; the integrand drops to half its central value at $y = {\cdot}19$ (NE), or ·16 (NW) while the graph corresponding to the case of spherical symmetry gives $y = {\cdot}31$. This means that the high-latitude contribution originates in a relatively narrow zone around the polar axis. Accordingly, the values of N in Table 5B have to be increased by about 30 per cent.

The results shown by Table 6 are not very illustrative because they show a mixture of two effects: the change of density with latitude and with increasing distance from the centre. I have tried to eliminate the latter effect by reducing all results to a common distance, $r = 1{\cdot}15$. Of course, this might be done rigorously by a much more elaborate photometry, involving horizontal tracings at all values of z. It was thought sufficient, however, to reduce the values of K in Table 6 proportionally to the functions $K(r)$ shown in Table 2, or 5 A, B, and the values of J proportionally to the functions $N(r)$ shown in Tables 5A, B. The value $r = 1{\cdot}15$ was chosen in order to have a reduction factor near 1 in the most interesting part, from $\beta = 80°$ to 60°. No appreciable difference was found if the polar or equatorial gradients were used as a basis for the reduction. The average values for the equatorial regions were taken directly from Table 5A. Inspection of the calibration curves mentioned in section 3 showed that, on the average, the brightness at $\beta = 0°$ was 9 per cent above, and the brightness at $\beta = 30°$ was 7 per cent below the assumed value. All points so obtained are shown in Figures 7A and B and free-hand curves have been drawn as a suggestion of the general behaviour. The values of N were computed from the corresponding values of J by means of

$$N = 9{\cdot}6.\ 10^5\, J, \tag{36}$$

following from equation (35) by substitution of $b = 1{\cdot}07$, $2A + B = 0{\cdot}97$.

The results of this section may be summarized as follows. The solution shown in Table 5B is not correct because there is no spherical symmetry. This is brought out clearly by the plot of the surface brightness (Figure 7A). It shows the general rise of the surface brightness for latitudes smaller than 65° and also a distinct dip near $\beta = 70°$. The resulting electron densities show similar, but more prominent, effects. The dip becomes very pronounced, going down to 10 or 20 per cent of the equatorial density and there is a peak at the pole of about half the equatorial density. The values of N for the polar axis, given in Table 5B, have to be increased by about 30 per cent near $r = 1{\cdot}1$. The correction at larger r is probably smaller, because the spreading of the polar rays tends to establish spherical symmetry. The values of p (and b) in Table 5B are virtually correct for all values of r.

FIGURE 7 A, B.

True surface brightness of the corona in minimum phase at the projected radius, $r = 1{\cdot}15$, as a function of heliographic latitude.

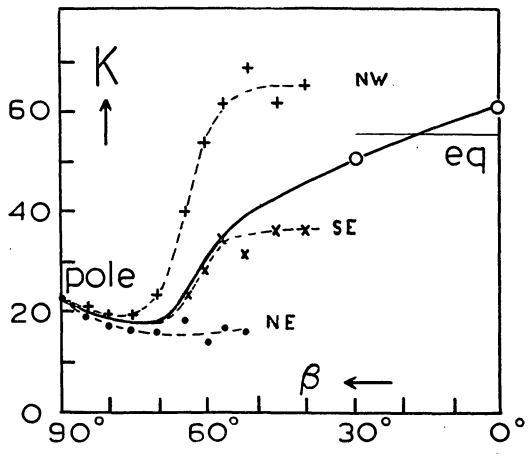

Electron density of the corona in minimum phase at the distance $r = 1{\cdot}15$ from the centre, as a function of heliographic latitude.

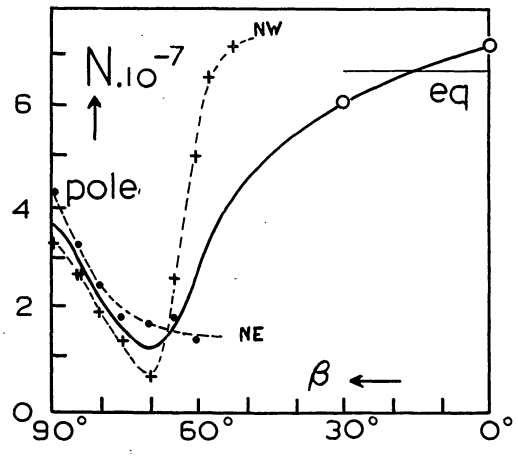

Casual inspection of a photograph, or an isophotal map, does not show the dip at $\beta = 70°$ as a prominent feature of the corona. Several effects conceal it: the superposition of the F-corona, the tendency of the steep outward gradient to make all isophotes circular and, finally, the fact that it becomes most pronounced only after the integral equation (29) has been solved. Figure 7B very strongly suggests that there are two agents responsible for the coronal activity in minimum phase: one operating near the pole and one operating in the equatorial regions up to latitudes of 60 degrees.

It is tempting to speculate about the relation between the phenomenon just found and other data on solar activity. In drawing the following outline I have had much use of a brief but excellent review by NICOLET[1]).

After the classical work on the form of the corona by LUDENDORFF[2]), the problem was further studied by BERGSTRAND[3]), who tried to eliminate the effect of the equatorial streamers projected on the polar regions. This problem is the same as treated above, but much of the 'veil' discussed by BERGSTRAND must be the F-corona and, moreover, his formulae are too schematic. Yet his work has the advantage of covering many eclipses and the results show a striking parallelism between the behaviour of the polar corona and the high-latitude prominences. That in particular the high-latitude, and not the low-latitude prominences have something to do with the coronal forms was already noted by LOCKYER[4]). It also was confirmed by the fact that the maxima of these phenomena in the eleven-year cycle are shifted with respect to the maxima of the sunspots in a similar way[1]).

The distribution in heliographic latitude is not at all similar, however. The high-latitude prominences[2]) concentrate about latitude 50° to 60° and are virtually absent at the poles. The emission lines of the corona show much the same effects[3]): a maximum in the main sunspot zone near 20°, a secondary maximum near 60°, and a very low value near the poles. This statement holds for the inner corona, $r < 1{\cdot}20$[4]). The 'chromospheric heights', though less well observed, exhibit the same tendency[5]), if we just remember that a low chromospheric height in general corresponds to high prominence activity. In sharp contrast to all of these phenomena is the electron density of the inner corona, as found above for one eclipse. It shows a fairly high value near the poles and a distinct minimum near $\beta = 70°$. This deviating behaviour is very puzzling. Different eclipse photographs should be studied in the same manner.

6. *Comparison with the Observed Polarization.*

The 'model corona' constructed in sections 3 and 4 consists of a list of values of the brightness, electron density, and polarization, of the K-corona and of the brightness of the F-corona. These values are mutually consistent within one per cent (except for the revision of the electron density on the polar axis in section 5, which, however, did not affect p). In order to judge whether these values agree also with the observations, we have to consider observational data on (*a*) total

1) M. NICOLET, *Ciel et Terre* **59**, 266, 1943.
2) H. LUDENDORFF, *Sitzungsber. Preuss. Ak. d. Wiss.* **10**, 185, 1928; **16**, 200, 1934.
3) Ö. BERGSTRAND, *Arkiv f. Mat. Astr. och Fysik* **22A**, No. 1, 1930, **25A**, No. 4, 1937, and *M. N.* **95**, 436, 1935.
4) W. J. S. LOCKYER, *M. N.* **82**, 323, 1922; **91**, 908, 1931.

1) G. ABETTI, *Publ. R. Oss. Arcetri* **56**, 53, 1938; M. BIOZZI, *ibidem* **57**, 5, 1939.
2) V. BAROCAS, *Ap. J.* **89**, 486, 1939.
3) M. WALDMEIER, *Z. f. Ap.* **21**, 85, 1941.
4) M. WALDMEIER, *Z. f. Ap.* **21**, 120, 1942.
5) M. G. FRACASTORO, *Publ. R. Oss. Arcetri* **64**, 44, 1948.

intensity, (*b*) surface brightness, (*c*) polarization, and (*d*) the depth of Fraunhofer lines.

Data on (*a*) and (*b*) have been used in constructing the model and are therefore in reasonable agreement with it. The discussion by ÖHMAN[1]) for the 1945 eclipse and a more general investigation by ALLEN[2]) have shown that the idea of a superposed K- and F-corona also qualitatively accounts for the typical features of data (*c*) and (*d*). The more quantitative discussion made below confirms these investigations in most respects, but reveals some interesting discrepancies. They may only partly be explained from the fact that coronae observed at the same phase of the solar cycle still show large individual differences.

Figure 8 gives a selection of observational data, together with new theoretical curves. The dashed curves represent the polarization of the K-corona (Table 5A, B). The full curves were obtained by multiplying these values by the factors f (Table 2). According to equation (3) these curves represent the degree of polarization of the combined F- + K-corona, on the assumption that the F-corona is unpolarized. The measurements by YOUNG[1]) (eclipses 1901, 1905 and 1908), FESSENKOFF[2]) (eclipse 1914) and COHN[3]) (eclipses 1932 and 1934) were taken from the compilation by BAUMBACH[4]). These measurements together with those by ALLEN[5]) (eclipse 1940) and VASHAKIDSE[6]) (eclipse 1941), were made photographically and may be given equal weights. The photo-electric determinations by HURAHATA[7]) (eclipse 1943) and the photographic determinations by ÖHMAN[8]) (eclipse 1945), who used four instruments simultaneously, probably have higher weights. I excluded from this compilation the data obtained by DUFAY-GROUILLER[9]) with not entirely adequate equipment (see also the criticism by HURAHATA), the visual measurements by JOHNSON[10]), and the obviously poor determinations by ZAKHARIN[11]).

FIGURE 8

Observed and computed polarization as a function of the distance from the sun's centre. Dashed curves: computed values of p_K; full curves: computed values of p for the combined F- and K-components. Small symbols: observed points, as indicated.

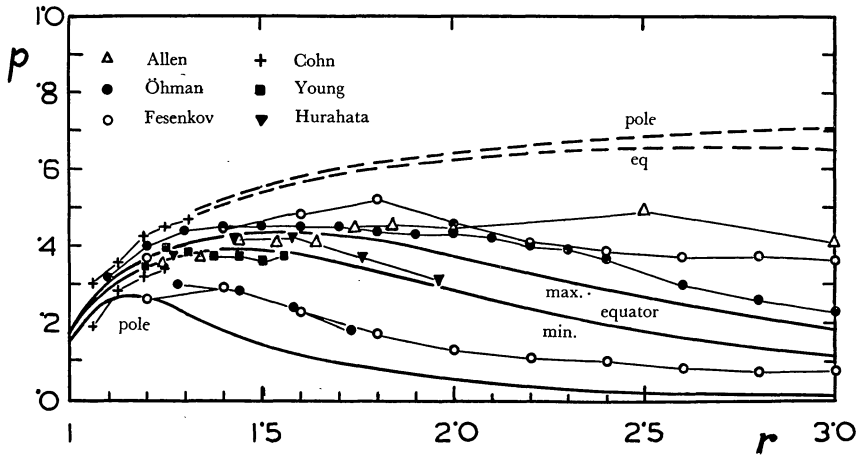

In broad lines, Figure 8 shows a satisfactory agreement between theory and observations. Both show that p drops gradually, after an initial rise to about 40 per cent, and that p is much lower near the pole. So the hypothesis of ÖHMAN and ALLEN, that the F-component is chiefly responsible for the deviation of the observed points from the dashed curves, is well confirmed. Yet the quantitative agreement is poor. We shall discuss various parts of the corona in more detail.

Equator regions, inner corona ($r < 1{\cdot}5$). Here the agreement is good. This is chiefly a check on the values p_K, for the F-corona has little influence. The model gives values for $f = K/(K + F)$ ranging from 0·87 to ·70 in the interval $r = 1{\cdot}3$ to $1{\cdot}5$. The measured p gives by means of equation (3) values between 1·00 and 0·67, with only two points higher than 0·90. So the adopted values of F seem all right, with an uncertainty of some 30 per cent either way. There is a small color effect in this region (not shown by the figure). I quote from HURAHATA that p_{blue} is 2 per cent higher than p_{red},

1) *Stockholm Ann.* **15**, No. 2, 1947.
2) *M. N.* **107**, 426, 1947.

1) R. K. YOUNG, *Lick Obs. Bull.* **6**, 166, 1911.
2) B. FESSENKOFF, *Russ. Astr. J.* **12**, 309, 1935.
3) W. H. COHN, *Ap. J.* **87**, 284, 1938.
4) *Astr. Nachr.* **267**, 273, 1939.
5) C. W. ALLEN, *M. N.* **101**, 281, 1941.
6) M. A. VASHAKIDSE, *Abastumani Bull.* **7**, 1, 1943 (see also **8**, 117, 1945).
7) M. HURAHATA, *Jap. J. Astr. Geophys.* **21**, 173, 1947.
8) *L. c.*
9) J. DUFAY and H. GROUILLER, *Lyon Publ.* **2**, 129, 1936.
10) J. J. JOHNSON, *P. A. S. P.* **46**, 226, 1934.
11) K. G. ZAKHARIN, *Abastumani Bull.* **3**, 72, 1938.

near $r = 1{\cdot}5$, in perfect agreement with MINNAERT's and BAUMBACH's calculations. The difference vanishes for larger distances from the sun, as shown convincingly by ÖHMAN's observations.

Equator regions, medium and outer corona ($1{\cdot}5 < r < 3{\cdot}0$). Here a pronounced difference between theory and observations is seen: the theoretical curves seem altogether too low. The difference is so strong that the more subtle difference of nearly 10 per cent between the predicted polarizations from the maximum and minimum phase seems unimportant. Let us discuss for convenience the interpolated values for $r = 2{\cdot}5$. The adopted values of f for the model are 0·40 (max) and 0·28 (min). The values determined from the depth of Fraunhofer lines are 0·22 to 0·35 (GROTRIAN[1]), eclipse 1923, minimum phase) and 0·41 (ALLEN[2]), eclipse 1940, intermediate). The agreement is good, because the model was based on these observations. The f computed from the measured p and the theoretical p_K, by means of equation (3), is much higher. ALLEN's point gives $f = 0{\cdot}75$ and the interpolated values for the two other sets are $f = 0{\cdot}51$ and 0·58. The difference with the adopted values is too large to be neglected. We may think of three explanations:

(*a*) The measured polarization is too high. This explanation receives some support from the fact that the only photo-electric measures (HURAHATA) do not deviate from the theoretical curves. These are the only measures from which the sky light was eliminated by direct measurement and where mean errors of the resulting p are given (ranging from 0·5 to 3 per cent). The correction for sky light (and plate fog) is much more difficult in photographic measurements. Sky light originates from the illumination of the sky by the sunlit regions of earth and air outside the eclipse cone; it must be fairly constant over the entire corona, including the dark of the moon. From HURAHATA's[3]) measures I compute that the sky light of an area 60 times the sun's area was 0·10 times the total light of the corona, i.e. about 60.10^{-8} times the sun's total light. The corresponding surface brightness is 0·10 in the units of Table 2. Five similar estimates, made by ALLEN[4]), range from 0·11 to 0·25 in the same units. HURAHATA points out that the amount may differ very strongly with weather conditions and with the duration of the eclipse.

The estimate 0·10 gives the sky light 1/5 of the intensity of the F-corona, at $r = 2{\cdot}5$. If it is polarized by $\pm$ 50 per cent, the estimated p of the combined light may range from 23 to 9 per cent, while it was 18 per cent without sky light. The difference is small, but the danger exists that the sky light was overestimated in the reductions. In other words, it seems possible that the observers have had a tendency to take part of the F-corona for sky light, or plate fog. The result is that the published values of p do not refer to the pure K-corona, nor to the combined light of K + F, but to something between. This is exactly what Figure 8 shows. This explanation is the most plausible one I can think of.

(*b*) The F-corona has some polarization of itself. In the equation,

$$p\,(F+K) = p_K K + p_F F,$$

we use the data $F = 0{\cdot}53$, $K = 0{\cdot}20$, and $p_K = 0{\cdot}65$, for $r = 2{\cdot}5$. But, instead of putting $p_F = 0$ and computing p, we now use the measured $p = 0{\cdot}54$ and compute p_F from the equation. We find $p_F = 0{\cdot}50$. In view of the assumed explanation of the F-component as a diffraction halo caused by interplanetary dust, such a degree of polarization seems impossible. So this explanation has to be rejected.

(*c*) The F-corona is less intense than estimated. The discrepancy noted in Figure 8 might simply mean that F was overestimated and f underestimated in the model. Using again equation (37), we have to keep the observed value of $F + K$ and $p_F = 0$, but we have to vary F and K until the correct p is obtained. Here is a complication: if K is increased in the outer corona, its outward gradient becomes less steep; consequently, p_K drops a little and consequently K has to increase even further in order that p attains the measured value. The way to avoid these subsequent approximations is to equate $p_K K$, which is the left-hand member of equation (20), to the measured product $p\,(K + F)$. By solving equation (20) and integrating equation (18) we find p_K and K separately. Table 7 gives a few values computed in this way from ÖHMAN's observations of p and the model values for $F + K$.

TABLE 7

Separation of F and K by the exclusive use of the observed polarization and total brightness (equator, minimum phase).

r	$F+K$	p	$p_K K$	
1·6	6·01	·45	2·70	
2·0	1·85	·43	·790	
2·5	0·73	·37	·272	
3·0	0·40	·28	·112	

r	K	p_K	f	f model
2·5	0·51	0·53	0·70	0·28
3·0	0·20	0·57	0·49	0·18

The value of f thus computed is much higher than that determined directly from the depth of Fraunhofer lines, on which also the model values were based. Referring to equation (2), we find that the actual depth

1) *Z. f. Ap.* **8**, 124, 1934.
2) *M. N.* **106**, 137, 1947.
3) *L. c.*
4) *M. N.* **107**, 426, 1947.